The Nucleus ***54***, *No. 4 (2017) 205-209*

www.thenucleuspak.org.pk

The Nucleus
ISSN 0029-5698 (Print)
ISSN 2306-6539 (Online)

Phase Evolution and Electrical Characterization of Bismuth Vanadate

Z. Tahir[1], M. U. Rashid[1] and S. Ahmad[2*]

[1]*Department of Physics, University of Peshawar, Peshawar, Pakistan*

[2]*Department of Physics, Islamia College Peshawar, Peshawar, Pakistan*

ARTICLE INFO

Article history :
Received : 02 March, 2017
Accepted : 22 December, 2017
Published : 31 December, 2017

Keywords:
BiVO4,
Ceramics,
Electrical properties

ABSTRACT

In the present study, phase, microstructure and electrical properties of $BiVO_4$ sample prepared by solid state sintering route have been studied. Phase analysis of the sintered sample revealed the formation of single phase $BiVO_4$ with no evidence of the secondary phase within the detection limit of X-ray diffractometer. Furthermore, the crystal structure has been investigated by Rietveld analysis which confirmed the monoclinic symmetry having lattice parameters a = 7.2478 Å, b = 11.695 Å, c = 5.0919 Å and β = 134.255°. SEM micrographs showed dense and irregular shaped grains with sizes ranging from 1.2 µm to 15.2 µm. Dielectric properties as a function of temperature for the $BiVO_4$ sample exhibited phase transition at three different temperatures (~69°C, ~280°C and ~465°C). The dielectric loss increases with increasing temperature, indicating the semiconducting like features at higher temperatures which were further confirmed using impedance spectroscopy data.

1. Introduction

Bismuth vanadate, $BiVO_4$ (BV) has attained great attention due to its use as non-toxic yellow pigment in paint film, coating process, low cost and stability. It is also used in a number of applications, e.g., gas sensors, posistors, solid state electrolyte and positive electrode material for lithium rechargeable batteries. Glasses of BV can be used in memory switching devices and electrical rectifiers as these have a peculiar non-ohmic behaviour beyond a threshold voltage. BV is also known to be a good photo-catalyst for water splitting and pollutant decomposing under visible light irradiation [1-4]. Naturally, BV occurs in brown colour as pucherite mineral; however, this form cannot be prepared using laboratory routes [5, 6]. BV prepared in the laboratory has light yellowish colour and can be formed in three different structures, namely (i) tetragonal zircon-type structure having space group $I4_1/amd$ [7], (ii) high temperature tetragonal scheelite structure having space group I2/a [7, 8] and (iii) monoclinic scheelite structure having space group $I4_1/a$ [7]. Phase transition is one of the most remarkable phenomena observed in BV. Several phase transitions above room temperature have been reported previously such as ferroeleastic to paraelastic phase transition [8-11].

In the present study, BV has been synthesized using solid state reaction route and characterized by using various techniques like X-ray diffraction (XRD), scanning electron microscopy, dielectric measurements and impedance spectroscopy.

2. Experimental Methods

BV has been prepared by mixed oxide solid state reaction route. The stoichiometric amount of Bi_2O_3 and V_2O_5 as a starting material were weighted according to the chemical formula:

$$Bi_2O_3 + 2BiVO_4 \rightarrow 2BiVO_4$$

The batch composition was mixed/milled in an agate mortar and pestle. The powders were sieved using a 300 pm mesh size, in order to dissociate agglomerates. After sieving, the dried mixture was then placed in alumina crucible inside a furnace at 600°C for 4h with a heating/cooling rate of 5°C/min. The calcined powders were re-milled using pestle and mortar. The main purpose of re-milling was to remove agglomerates and reduce the particle size to enhance the sinterability. The re-milled calcined powders were pressed into cylindrical shaped pellets using a 10mm steel die by applying a pressure of 100MPa.The thickness of the pellets was 3-5 mm while its diameter was 10 mm (before sintering).The pellets obtained were then sintered at 800-850°C for 2h at a heating/cooling rate of 5°C/min.

XRD data of BV powder sample was collected using D5000 Siemens X-ray diffractometer (Germany), with CuKα radiation source. Phase analysis has been carried out using Winxpow software. Microstructure analysis of finely polished, thermally etched and gold coated BV sample was performed using JEOL JSM-5910 scanning electron microscope (SEM) operated at 30kV. Impedance spectroscopy of BV sample was performed using an impedance analyzer (Agilent E4980A) over a frequency range from 20 Hz to 2 MHz in a temperature range of 250 to 500°C. Dielectric permittivity and dielectric losses at 100

*Corresponding author : arbab.safeer@icp.edu.pk

kHz, 250 kHz and 1 MHz were measured using a precision LCR meter (HP-4287A) with an applied voltage of 100 mV in the temperature range 25 to 500°C in air. Dielectric constant and tanδ of the sample were calculated using equation (1) and (2), respectively.

$$\varepsilon_r = \frac{Cd}{A\varepsilon_o} \quad (1)$$

$$tan\delta = \frac{\varepsilon'}{\varepsilon''} \quad (2)$$

Where C, d, A and ε_o represent capacitance, thickness, area for the sample and permittivity of free sample, respectively. In equation (2), ε' is real part and ε'' is imaginary part of permittivity.

3. Results and Discussions

X-ray diffraction pattern of BV ceramics sintered at 820°C is shown in Fig. 1. The interplaner spacing and the relative intensities recorded for BV sample matched with the PDF card # 14-688, having monoclinic (C12/c1) symmetry. The sample revealed a single-phase perovskite structure with no evidence of any secondary phase formation. The refined lattice parameters using Rietveld method are; a = 7.2478 Å, b = 11.695 Å, c = 5.0919 Å and β = 134.255°. The atomic positions, occupancy factors and Wyckoff positions are given in Table 1. The relative intensity and d-spacings are listed in Table 2.

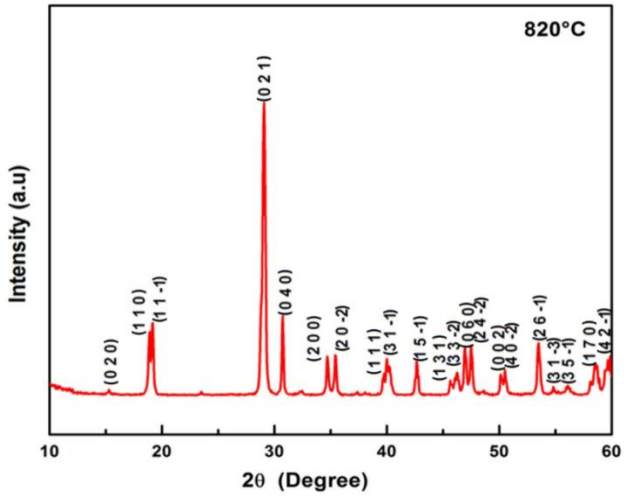

Fig. 1: X-ray diffraction pattern of BV sintered at 820°C

SEM micrograph of polished and thermally etched BV sample sintered at 820°C for 2h is shown in Fig. 2 which reveals dense microstructure with grains of irregular morphologies, varying in lengths between ~1.2 to ~15.2 µm.

Dielectric constant Vs temperature data for BV sample at various frequencies (100 kHz, 250 kHz and 1 MHz) is shown in Fig. 3. The first peak at 69°C may refer to the phase transition, however, further proof is required to confirm changes in symmetry (if any) using in-situ XRD or Raman spectroscopy. The second peak is associated with the reversible phase transition from monoclinic scheelite to tetragonal scheelite with a change in the space group from I2/a to $I4_1/a$ at 280°C. Similarly, the third peak corresponds to the irreversible phase transition from tetragonal zircon to monoclinic scheelite at ~465°C [7]. The dielectric loss is minimum at room temperature (0.015 at 1MHz), but increases with increase in temperature indicating a semiconducting behaviour as shown in Fig. 4, which is further confirmed using impedance spectroscopy.

Table 1: Crystallographic data of BV

Atoms	Occupancy	Atomic fraction	Coordinates		
			X	Y	Z
Bi 1	4e	1.000000	0.000000	0.633043	0.250000
V 1	4e	1.000000	0.000000	0.124880	0.250000
O 1	8f	1.000000	0.131347	0.202272	0.156343
O 2	8f	1.000000	0.273646	0.446393	0.388(8)

Table 2: Glancing angle (2θ), planes and relative intensity

No	2θ	*H*	*K*	*L*	Intensity
1	18.8489	1	1	0	22.77
2	18.8958	1	1	0	21.08
3	19.1567	1	1	-1	28.63
4	19.2043	1	1	-1	26.61
5	28.7750	1	3	0	19.23
6	28.8477	1	3	0	26.56
7	28.9819	1	3	-1	82.02
8	28.9900	0	2	-1	85.96
9	28.9900	0	2	1	85.96
10	29.0550	1	3	-1	99.61
11	29.0631	0	2	-1	100.00
12	29.0631	0	2	1	100.00
13	29.1298	2	2	-1	96.58
14	29.2033	2	2	-1	67.81
15	30.7127	0	4	0	22.42
16	30.7905	4	0	4	18.76
17	34.6905	2	0	0	14.52
18	34.7790	2	0	0	11.56
19	35.3857	2	0	-2	13.33
20	49.9243	2	4	0	15.51
21	47.0474	2	4	0	11.19
22	47.4675	2	4	-2	15.36
23	53.4040	0	6	-1	13.36
24	53.4040	0	6	-1	13.36
25	53.4883	2	6	-1	16.05
26	53.5457	0	6	-1	14.30
27	53.5457	0	6	-1	14.30

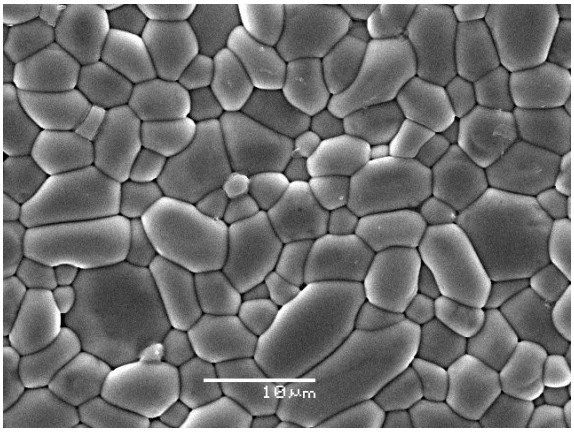

Fig. 2: Secondary electron micrograph (SEM) of BV sintered at 820°C

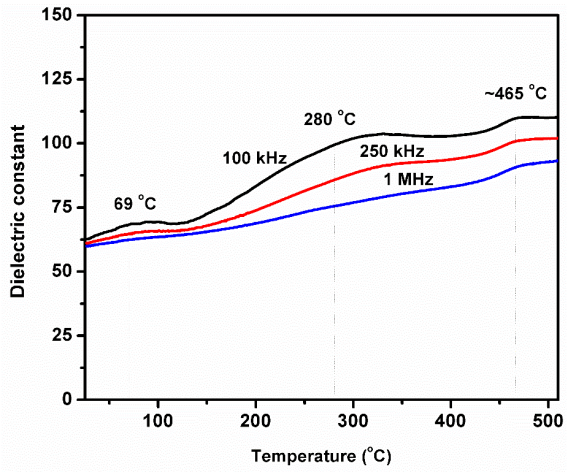

Fig. 3: Dielectric constant vs temperature curve

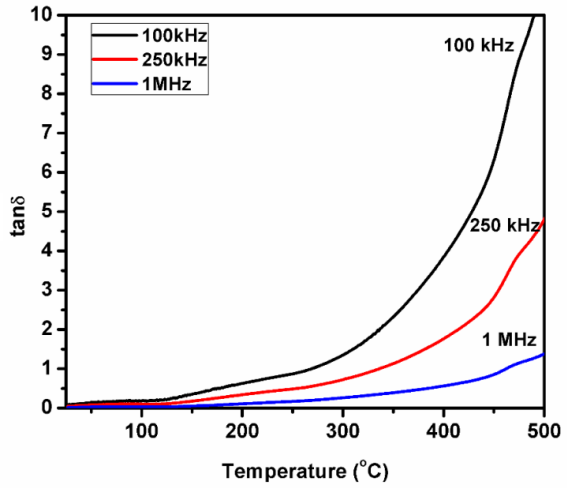

Fig. 4: Dielectric loss vs temperature curve

Impedance spectroscopy is a convenient and powerful technique for the characterization of a wide range of electrical properties of electro-ceramics. It has a great advantage of separating the electrical response of different regions of ceramics according to their relaxation times or time constants [12-14].

Fig. 5 shows the impedance plane plot at various temperatures (265°C, 345°C, 400°C, 455°C, and 500°C). A single semi-circle arc appeared at 265°C, which decreases in radius with increasing temperature indicating a semiconducting behaviour consistent with dielectric loss data (Fig. 4).

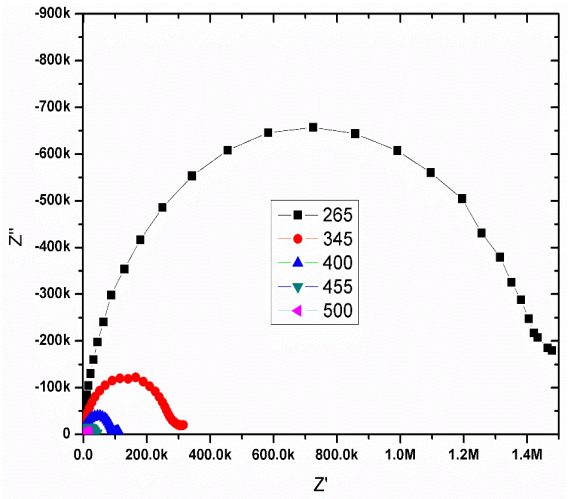

Fig. 5: Impedance plane plot (Z″ vs Z′)

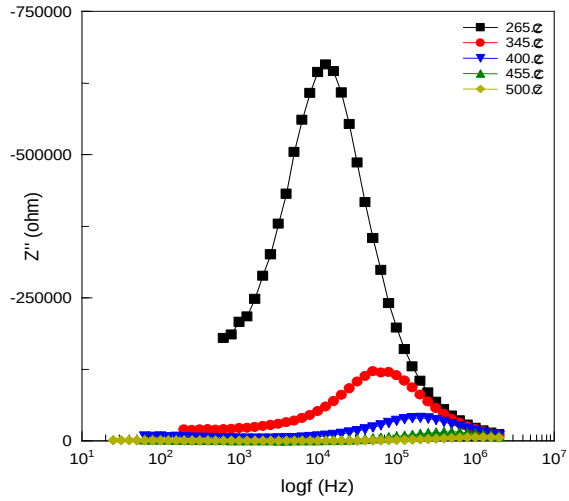

Fig. 6: Spectroscopic plot of Z″ vs log(f)

The spectroscopic plots (log(f) Vs Z″) and (log(f) Vs M″) are presented in Figs. 6 and 7, respectively, show a single peak at all measured temperatures (265°C, 345°C, 400°C, 455°C, and 500°C). From the peak maximums, resistance and capacitance values were determined using the following equations:

$$R = 2Z^{"} \quad (3)$$

$$2\pi f C R = 1 \quad (4)$$

$$C = \frac{\varepsilon_o}{2M^{"}} \quad (5)$$

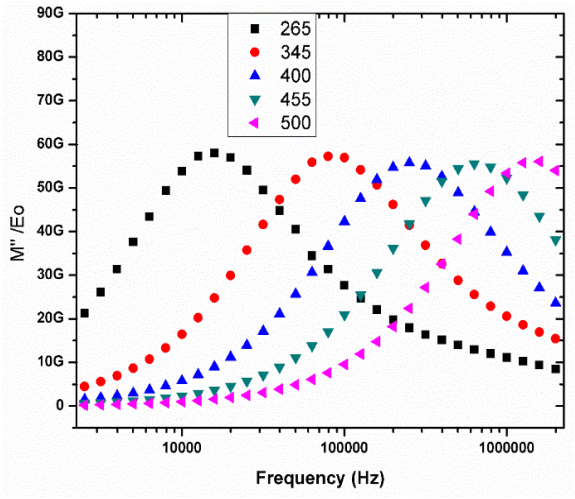

Fig. 7: Spectroscopic plot of M″ vs log(f)

The capacitance and resistance values calculated from Figs. 6 and 7 are summarized in Table 3. The capacitance values are in the range of Pico farad (pF) and can be associated to the bulk (grain), according to the criteria proposed by Irvine et al. [13]. The slight difference in the values of R_g and C_g obtained from Z″ and M″ is indicative of electrical heterogeneity. To resolve this ambiguity, capacitance plot i.e. log(*f*) Vs log(C) (Fig. 8) at various temperatures has been taken into account. From Fig. 9 which is an Impedance plane plot (Z″ Vs Z′), it can be seen that at higher frequencies, the existence of the bulk region is clear but at lower frequencies there is an indication of grain boundary region and electrode effect as well which is in contradiction with the spectroscopic plots, presented in Figs. 6 and 7, where there is no evidence of grain boundary and electrode effect peak. The reason for this discrepancy may be the limited frequency range of the instrument.

Table 3: Values of R and C extracted from Z''_{max} and M''_{max}

Temp (°C)	R_g	C_g	R_g	C_g
	Extracted from Z″		Extracted from M″	
265 °C	1.31×10^{6}	9.62×10^{-12}	1.17×10^{6}	8.61×10^{-12}
345 °C	2.40×10^{5}	8.33×10^{-12}	2.29×10^{5}	8.74×10^{-12}
400 °C	8.04×10^{4}	9.92×10^{-12}	7.07×10^{4}	8.96×10^{-12}
455 °C	3.01×10^{4}	8.23×10^{-12}	2.80×10^{4}	8.99×10^{-12}
500 °C	1.36×10^{4}	9.31×10^{-12}	1.13×10^{4}	8.92×10^{-12}

The conclusion of this impedance spectroscopy analysis is that the first semi-circle arc in the impedance plane plots (Z′ Vs Z″) corresponds to the bulk region while the quarter portion of the second semi-circle might corresponds to the combined grain boundary region and electrode effect as shown in Fig. 9. This may be due to the overlapping of two electroactive regions with very close conductivities

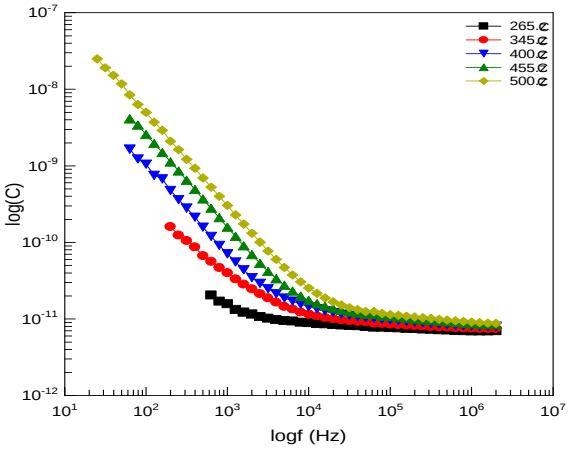

Fig. 8: Capacitance plots log(C) Vs log(f)

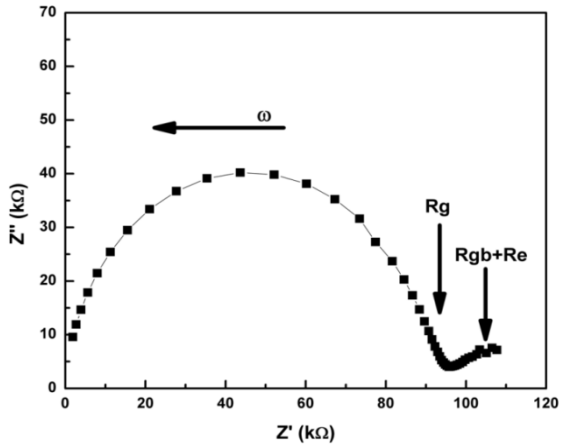

Fig. 9: Impedance plane plot (Z″ Vs Z′)

which needs further investigation at low temperatures which can give us more information about the investigated sample, especially about the electrode effect. A more conventional method of presenting resistance (or conductivity) data is an Arrhenius plot against the reciprocal of temperature (Fig. 10). The activation energy corresponding to the bulk or grain region for BV sample is 0.69 eV which has been obtained from Arrhenius plot (Fig. 10).

4. Conclusions

BV sample was prepared via conventional solid state sintering route. XRD analysis confirmed that BV sample sintered at 820°C has monoclinic (C12/c1) structure. Dense microstructure with grains of irregular shaped different sizes ranging from 1.2 to 15.2 µm has been observed. Dielectric constant Vs temperature curve measured at different frequencies (100 kHz, 250 kHz and 1 MHz), indicated three different phase transitions at ~69°C, ~280°C and ~465°C while the dielectric loss Vs temperature curve showed an increase in the dielectric loss with increase in the temperature. Impedance spectroscopy analysis of BV sample shows the presence of grain or bulk region having activation energy of 0.69 eV.

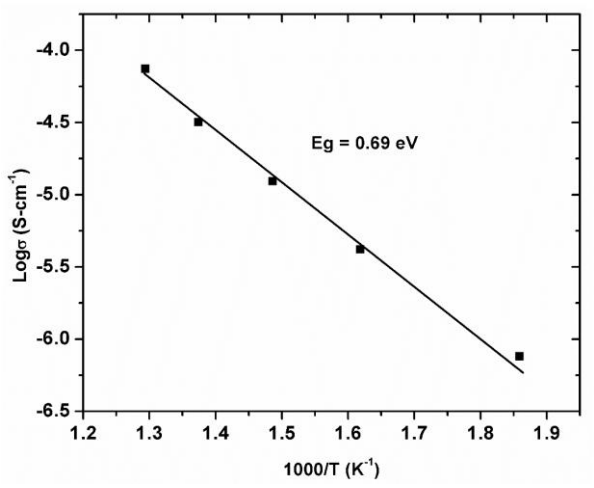

Fig. 10: Arrhenius plot for grain or bulk region

References

[1] D. Barreca, L. Depero, V.D. Noto, G. Rizzi, L. Sangaletti and E. Tondello, "Thin films of bismuth vanadates with modifiable conduction properties", Chemistry of Materials, vol. 11, pp. 255-261, 1999.

[2] M.C. Neves, T. Trindade, "Chemical bath deposition of $BiVO_4$", Thin Solid Films, vol. 406, pp. 93-97, 2002.

[3] T. Yang, D. Xia, "Self-assembly of highly crystalline spherical $BiVO_4$ in aqueous solutions", Journal of Crystal Growth, vol. 311, pp. 4505-4509, 2009.

[4] L. Zhou, W. Wang, L. Zhang, H. Xu and W. Zhu, "Single-crystalline $BiVO_4$ microtubes with square cross-sections: microstructure, growth mechanism, and photocatalytic property", The Journal of Physical Chemistry C, vol. 111, pp. 13659-13664, 2007.

[5] A. Bhattacharya, K. Mallick, A. Hartridge, "Phase transition in $BiVO_4$", Materials Letters, vol. 30, pp. 7-13, 1997.

[6] R.L. Frost, D.A. Henry, M.L. Weier and W.N. Martens, "Raman spectroscopy of three polymorphs of $BiVO_4$: Cinobisvanite, dreyerite and pucherite, with comparisons to (VO4) 3-bearing-minerals: namibite, pottsite and schumacherite", Journal of Raman Spectroscopy, vol. 37, pp. 722-732, 2006.

[7] D. Zhou, L.-X. Pang, W.-G. Qu, C.A. Randall, J. Guo, Z.-M. Qi, T. Shao and X. Yao, "Dielectric behavior, band gap, in situ X-ray diffraction, Raman and infrared study on (1− x) BiVO 4–x (Li 0.5 Bi 0.5) MoO 4 solid solution", RSC Advances, vol. 3, vol. 5009-5014, 2013.

[8] M. Gotić, S. Musić, M. Ivanda, M. Šoufek and S. Popović, "Synthesis and characterisation of bismuth (III) vanadate", J.Molecular Structure, vol. 744, pp. 535-540, 2005.

[9] A. Zhang and J. Zhang, "Effects of europium doping on the photocatalytic behavior of BiVO 4", J.Hazardous Materials, vol. 173, pp. 265-272, 2010.

[10] J. Bierlein and A. Sleight, "Ferroelasticity in $BiVO_4$", Solid State Communications, vol. 16, pp. 69-70, 1975.

[11] S. Tokunaga, H. Kato and A. Kudo, "Selective preparation of monoclinic and tetragonal $BiVO_4$ with scheelite structure and their photocatalytic properties", Chemistry of Materials, vol. 13, pp. 4624-4628, 2001.

[12] E. Barsoukov and J.R. Macdonald, "Impedance spectroscopy: theory", experiment, and applications, John Wiley & Sons, 2005.

[13] J.T. Irvine, D.C. Sinclair and A.R. West, "Electroceramics: characterization by impedance spectroscopy", Advanced Materials, vol. 2, pp. 132-138, 1990.

[14] M. Amir, S. Atiq, S. Riaz and S. Naseem, "Effect of Ba-Substitution at Sr-Site on the Structural and Dielectric Characteristics of $SrMnO_3$", The Nucleus, vol . 52, pp. 155-158, 2015.